Supp.Fig.1. Mixed deficits among TTX-resistant muscle-type sodium channels in onset of inactivation despite identical kinetics and open-state probability

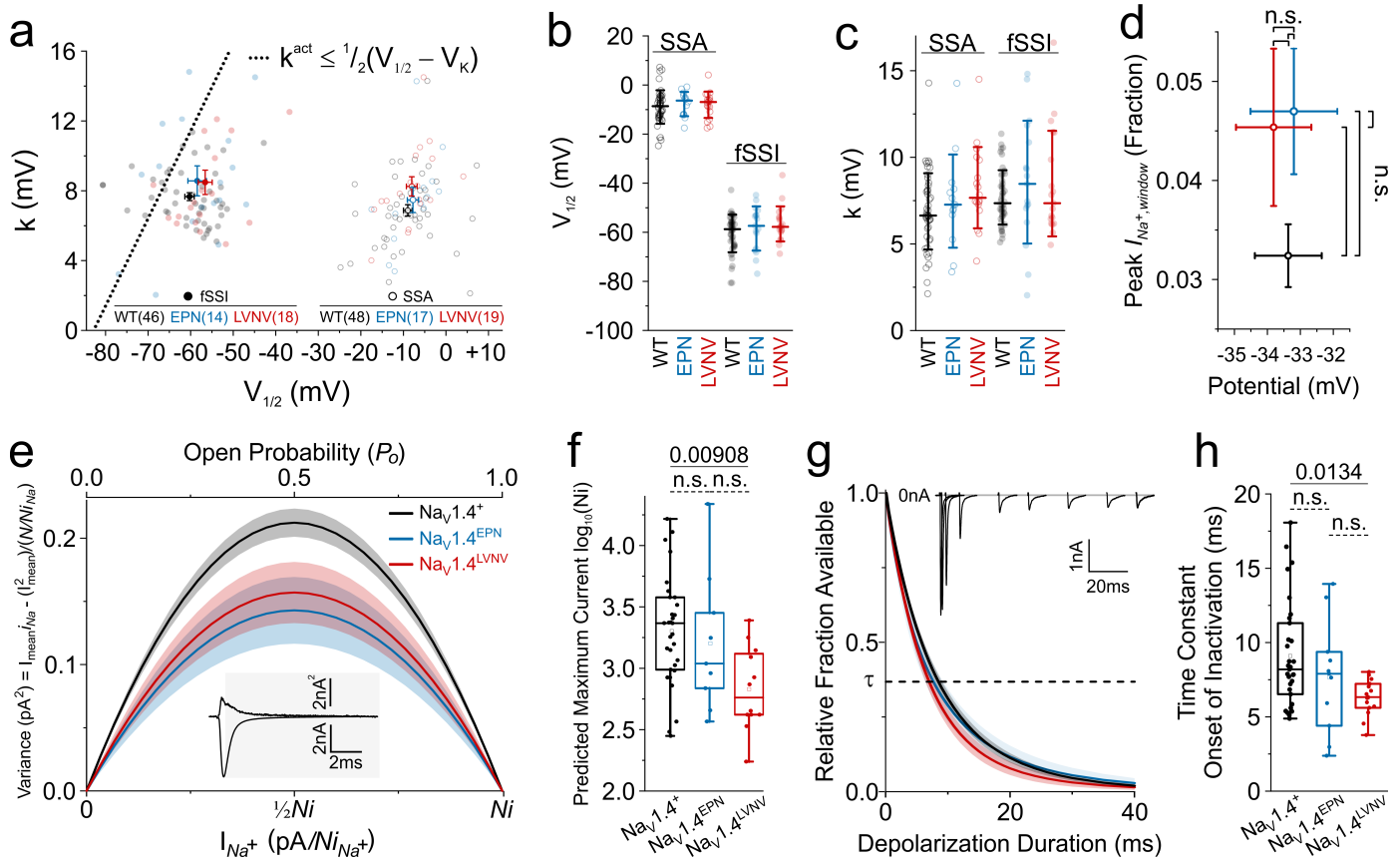

a, Steady-state activation (SSA, open circles) and fast inactivation (fSSI, closed circles) are within reasonable range for both TTX-sensitive (**$Na_V1.4^+$**, black) and TTX-resistant (**$Na_V1.4^{EPN}$**, blue and **$Na_V1.4^{LVNV}$**, red) skeletal muscle sodium channels, with average kinetics parameters falling well above the minimum threshold for excitability (dotted line). **b**, The voltage at half-maximal SSA and fSSI and the rate of change through that potential (**c**) are similar between resistant and sensitive channels. **d**, The average peak window current and voltage thereof are not significantly different between resistant and sensitive channel variants (average ± sem shown). **e**, Relative to the predicted maximum current (*Ni*) at the non-zero root of the parabola, there appear to be no differences in peak open probability despite reduced total conductance (Fig.1G,H). The inset represents a mean current-variance protocol with the grey background indicating the decay phase that produced parabolic current-variance. **f**, Despite the absence of any significant differences in total channel count (*N*) and any significant differences in unitary conductance between TTX-resistant channels, predicted maximum currents (*Ni*) only appear weaker between the **$Na_V1.4^+$** and **$Na_V1.4^{LVNV}$**, suggesting the triple point mutant may not be as costly, consistent with its greater macroscopic current. **g,** **$Na_V1.4^{LVNV}$** enters into the inactive state faster than **$Na_V1.4^+$**. The inset of **g** shows an example onset of inactivation protocol whereby the membrane is held at near peak window current potential (-40mV) for increasing durations, here called the *depolarization duration*, which precedes a test pulse at the top of the SSA curve (+10mV). **h**, The time constant of exponential current decay is significantly shorter in **$Na_V1.4^{LVNV}$** which is consistent with unique deficits found in snake skeletal muscle carrying this suite of mutations (Fig.2c). Values in **h** correspond to the time values observed at the point of level crossing with the dashed line (τ_{oofi}) in **g**. All p-values presented calculated by Dunn's post hoc pairwise comparison test after Kruskal-Wallis non-parametric ANOVA.